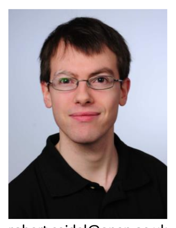

Hydrothermal Alteration in the Frankenstein Gabbro Martian Analogue

robert.seidel@open.ac.uk

R.G.W. Seidel[1], S.P. Schwenzer[1], J.C. Bridges[2] T. Kirnbauer[3], S.C. Sherlock[1]

[1]The Open University, UK. [2]University of Leicester, UK. [3]TH Bochum, Germany

Frankenstein Gabbro, Odenwald, Germany

1. Introduction

Hydrothermal systems on Mars are promising target sites in the search for potential (past) Martian life [1]. Their properties are not well known due to lack of samples available for detailed Earth-based study.

Model studies of hydrothermally-altered Martian meteorites indicate fluids habitable for microbial life (Fig. 1). However, these meteorites do not represent average – basaltic – Martian crust [2]. The habitability of basalt-hosted Martian systems remains uncertain.

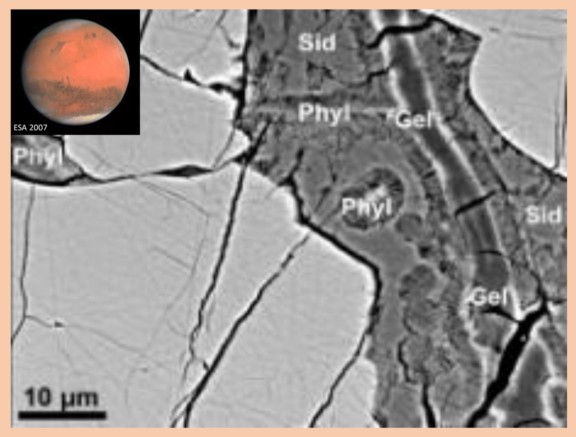

Fig. 1. Hydrothermal alteration in a Martian meteorite [after 3]. Models suggest a habitable late-stage fluid [4].

Name: Lafayette
Type: Nakhlite
Composition: Clinopyroxene cumulate
Formation age: ~ 1.3 Ga [5,6]
Alteration age: < 670 Ma [7]

Sid – siderite (Fe-carbonate)
Phyl – phyllosilicate (Fe-smectite & serpentine)
Gel – amorphous silica

Aim of this study: Predict hydrothermal alteration in basaltic host rocks on Mars through a terrestrial analogue model study.

- Constrain reaction paths by which primary minerals are replaced
- Specify expected properties of the hydrothermal fluid
- Identify proxy mineral assemblages indicating formerly habitable fluid conditions (T, P, pH, redox, nutrients)

Our research will provide information for target and sampling site selection of future Mars missions (e.g. Mars2020, ExoMars).

2. The Frankenstein Gabbro Martian Analogue

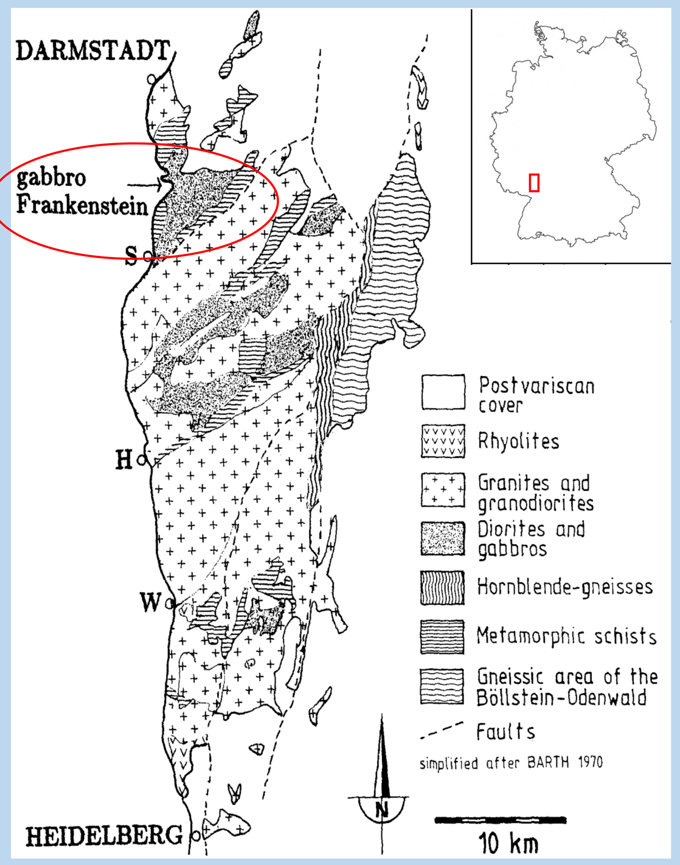

Fig. 2. Location of Frankenstein Gabbro in the Odenwald [8]. Insert showing location within Germany.

Locality: Odenwald, Germany (Fig. 2)
Type: Gabbro (chemical basalt-equivalent)
Pre-altered composition:

Plagioclase (~ 70 vol.%)
Clinopyroxene (~ 20 vol.%),
Amphibole (~ 9 vol.%)
Fe-oxide (1 vol.%)

Formation age: 360 Ma [8]

Multiple alteration events [9, 10], two observed in this study:

- Stage 1 (138 ± 8 Ma [9]) moderate, widespread, hairline faults and mineral veinlets.
- Stage 2 (undated) extensive, locally restricted, fault zones up to 1 m, calcite veins up to 10 cm.

Our study focuses on Stage 1:

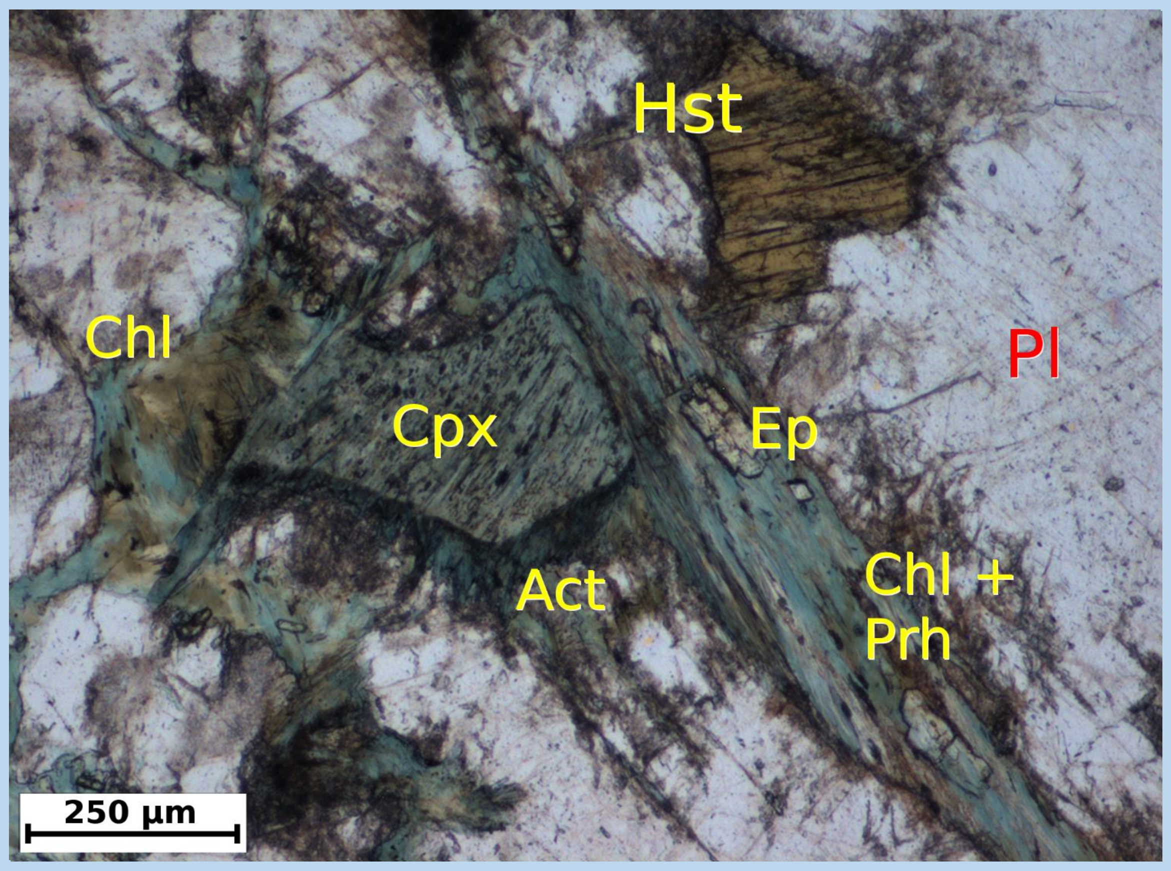

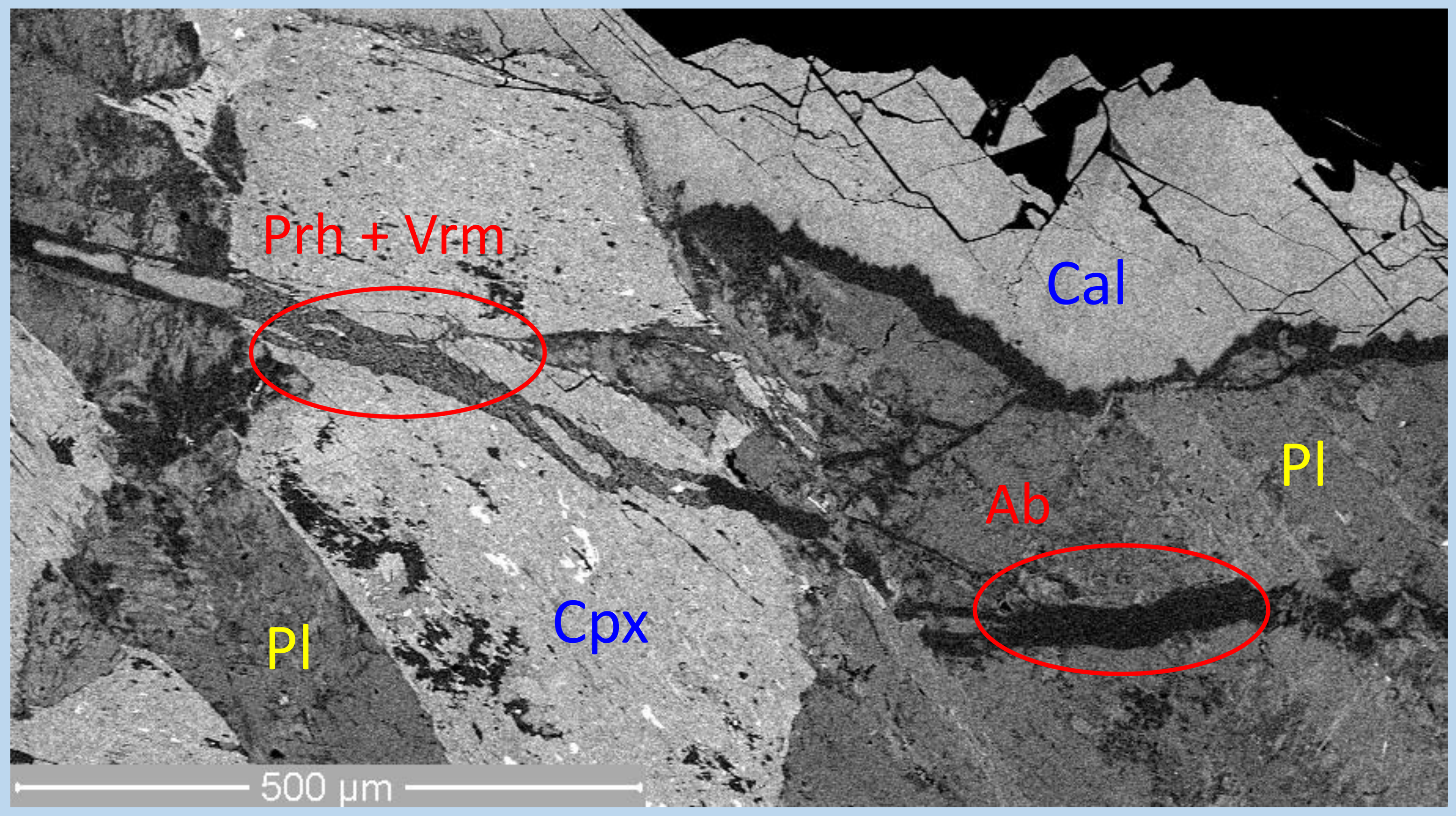

Fig. 3. Mineralogical features of alteration Stage 1. a) healed fault plane (chlorite-epidote-prehnite) and reaction seams around clinopyroxene (actinolite-chlorite). b) fluid veinlet showing small-scale variability, changing from albite within plagioclase host to prehnite-vermiculite within clinopyroxene host. **Abbreviations:** Ab – albite, Act – actinolite, Cal – calcite, Chl – chlorite, Cpx – clinopyroxene, Ep – epidote, Hst – hastingsite, Pl – plagioclase, Prh – prehnite, Vrm – vermiculite.

3. Alteration Stage 1

Time: 138 ± 8 Ma [9]

Tectonic features: Hairline fault planes (~ 100–250 µm)
Mineral veinlets (~ 25–100 µm)
Several cross-cutting generations (Fig. 4)

Complex secondary mineralisation, strong dependence on host mineral, strong small-scale variability (Fig.4-6):

Plagioclase host → Albite-epidote ± calcite ± chlorite ± K-feldspar
K-feldspar ± chlorite
Chlorite-epidote ± prehnite
Clinopyroxene host → Actinolite ± chlorite ± vermiculite
Prehnite-vermiculite
Amphibole host → Chlorite ± titanite

Dependence on water / rock ratio:

Fault planes (high W/R) typically chlorite-dominated
Veinlets (low W/R) typically plagioclase-dominated

Fig. 4. Relationship of fluid pathways formed during alteration Stage 1. Ovals show secondary assemblages modelled in Fig. 6.

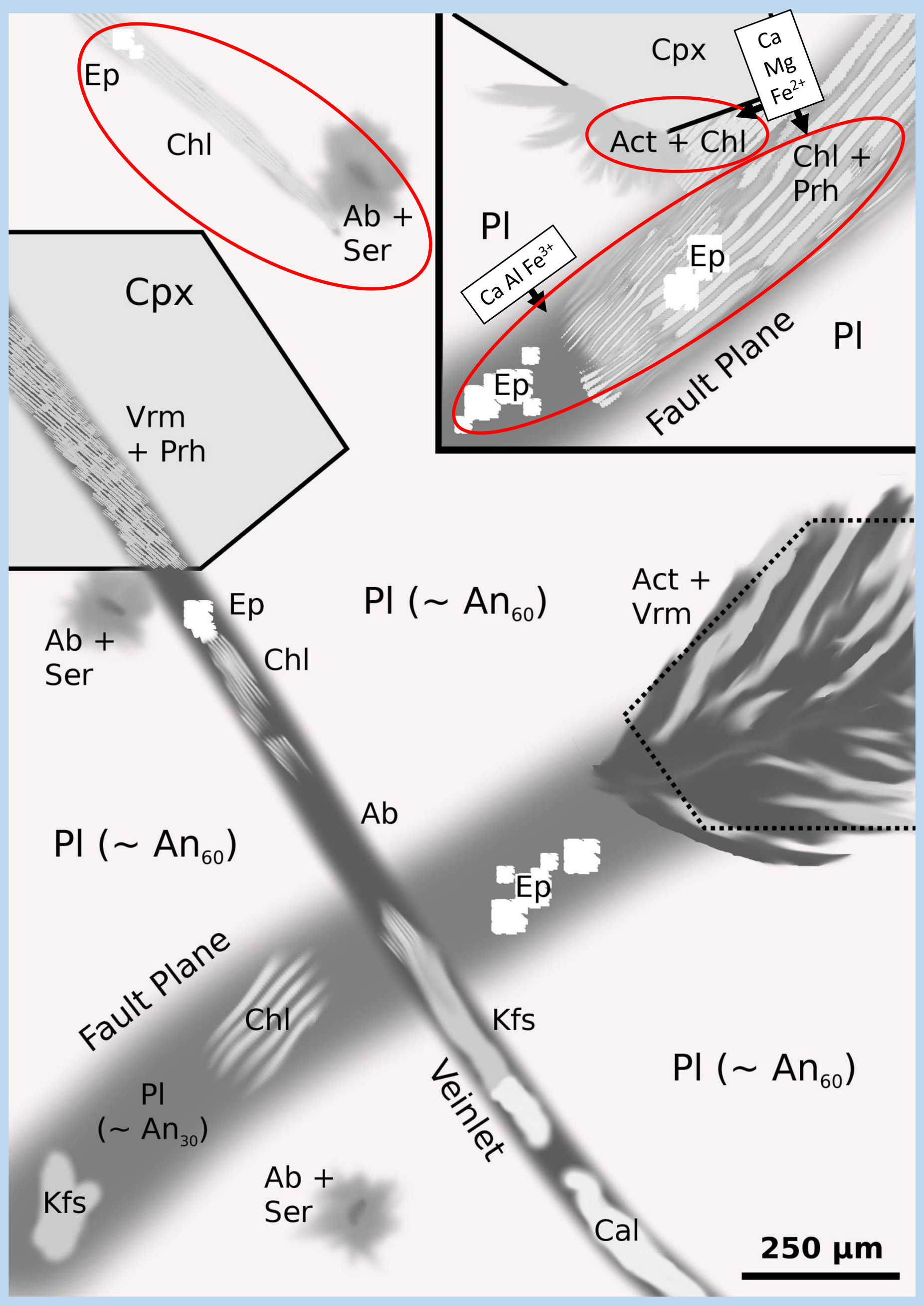

Pre-model constraints on fluid conditions:

Pressure: 1.5 km sediment cover at time of alteration implies hydrostatic pressure of 150 bars

Temperature: Presence of actinolite, epidote, prehnite suggests T > 250 °C [11]

pH: Mineral assemblage points to circumneutral conditions [11]

Composition: Observed quantities of primary and secondary minerals, and element budgets of replacement reactions, indicate influx of Na, K, Fe, Mg, Si from the fluid (Table 1)

Table 1. Element imbalance during alteration Stage 1, expressed as mMol per gram of reacting bulk rock.

mMol / g BR	K	Na	Ca	Fe	Mg	Al	Si
Consumed:	1.2	1.1	0.0	0.4	4.8	0.0	2.2
Released:	0.0	0.0	3.7	0.0	0.0	0.1	0.0

4. Results

By varying input composition (bulk rock, single minerals), temperature, and Fe^{2+} / Fe^{3+} ratio, we reproduce secondary mineral assemblages related to alteration rims around clinopyroxene (Fig. 6a) and fault planes (Fig. 6b). Pre-model observations are confirmed and refined:

- Temperature 250–275 °C
- pH ~ 6.5–8.0
- Chlorite dominating at high W/R
- Albite formed at low W/R (< 300)

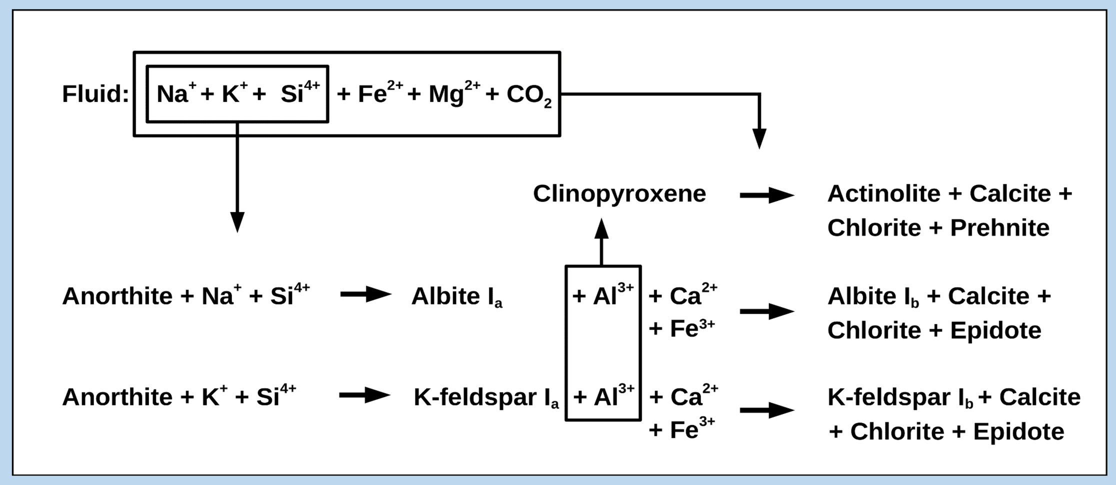

Fig. 5. Important mineral reactions during alteration Stage 1. Initial fluid composition based on Table 1, fluid conditions inferred from literature [10,11], and models shown in Fig. 6.

4. Results cont.

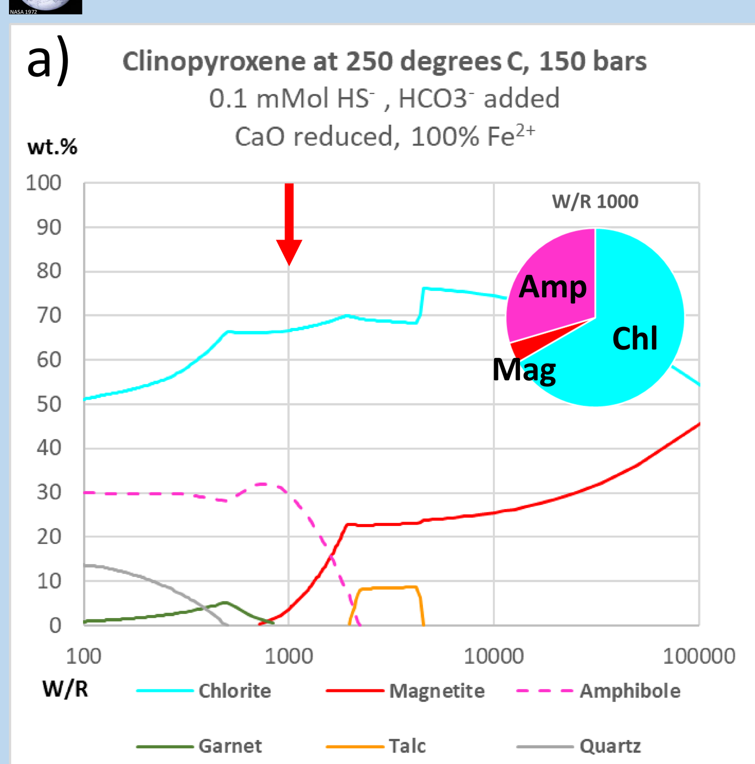

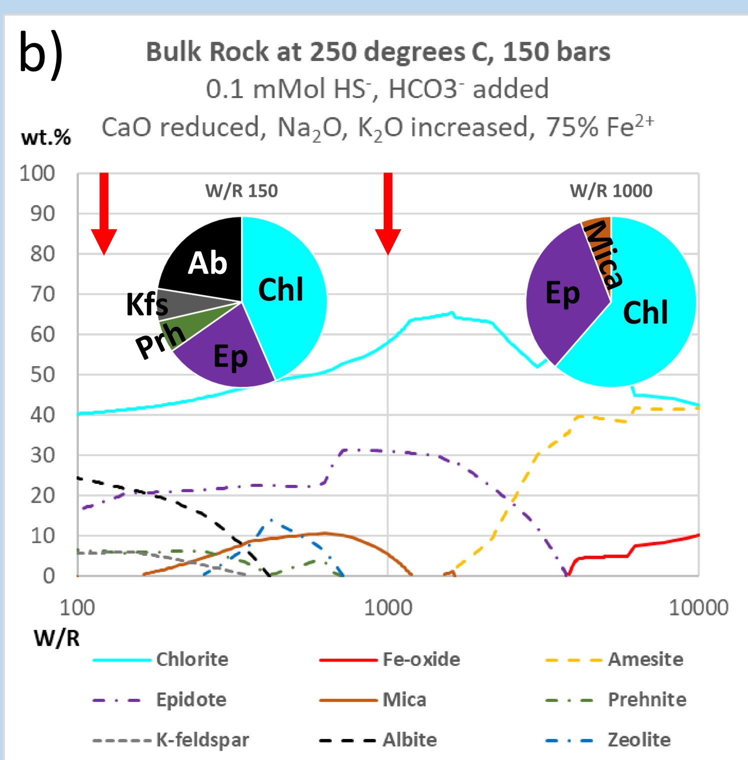

Method: Software CHIM-XPT [12]. Input: Published bulk rock XRF data [13], EMP mineral analyses, starting fluid with element ratios shown in Table 1.

5. Discussion

The models match and supplement key petrological observations, thus providing information about the alteration process beyond what may be directly observed:

- Loss of Ca, influx of Na, K during plagioclase alteration
- Calcite, vermiculite formed during late-stage cooling
- Secondary mineralisation strongly dependent on host minerals
- Redox state of host mineral influences redox state of fluid, e.g. Fe^{2+} released by clinopyroxene, Fe^{3+} by plagioclase (up to 0.5 wt.% in primary plagioclase)
- Local variability of dissolved Fe^{2+} / Fe^{3+} causes observed variability of chlorite, epidote, prehnite

Fig. 6. Results of CHIM-XPT model runs, reproducing secondary mineral assemblages shown within ovals of Fig. 4. a) model for clinopyroxene alteration, b) model for bulk rock alteration.

6. Conclusion & Outlook

Our models successfully constrain reaction paths and fluid properties during alteration of the Frankenstein Gabbro. They further illustrate the need to account for small-scale variability, and to adjust models on a case-by-case basis.

Similar small-scale variability of hydrothermal veinlets has been observed in Martian meteorites [3]. This has important implications for Martian habitability, as fluid properties may differ significantly even within the same vein.

Next, we will refine our models before applying them to Mars. We will particularly focus on small-scale distribution of dissolved iron species, a suggested energy source for hypothetical simple Martian life [e.g., 14].

References: [1] Farmer & Des Marais (1999) J. Geophys. Res. 104, 26, 977–995. [2] McSween et al. (2009) Science 324, 736–739. [3] Hicks et al. (2014) GCA 136, 194–210. [4] Bridges & Schwenzer (2012) EPSL 359–360, 117–123. [5] Nyquist et al. (2001) Chron. & Evol. Mars (Kluwer Publ.) 105–164. [6] Treiman (2005) Ch. d. Erde 65, 203–270. [7] Swindle et al. (2000) MAPS 35, 107–116. [8] Kirsch et al. (1988) Geol. Rdsch. 77, 3, 693–711. [9] Lippolt & Kirsch (1994) Geol. Jb. Hessen, 122, 123–142. [10] Burisch et al. (2017) Ore Geol. Rev. 81, 42–61. [11] Reyes (1990) J. Volc. Geoth. Res. 43, 279–309. [12] Reed et al. (2010) CHIM-XPT Users Guide. [13] Kreher (1994) Geol. Jb. Hessen 122, 81–122. [14] Price et al. (2018) Front. Microb. 9, #513.